



# PRODUCTION ENGINEERING ARCHIVES

ISSN 2353-5156 (print)  
ISSN 2353-7779 (online)

Exist since 4<sup>th</sup> quarter 2013  
Available online at [www.pea-journal.eu](http://www.pea-journal.eu)

## Mechanical and mathematical research of local deformations of a steel roller shell with a variable geometry of contact surface

Mikhail Doudkin<sup>1</sup>, Alina Kim<sup>2</sup>, Murat Sakimov<sup>3</sup>

<sup>1</sup> East Kazakhstan state technical university, Ust-Kamenogorsk, Kazakhstan, ORCID ID: 0000-0001-5732-0724, e-mail: Doudkin@mail.ru

<sup>2</sup> East Kazakhstan state technical university, Ust-Kamenogorsk, Kazakhstan, ORCID ID: 0000-0002-9332-4279

<sup>3</sup> East Kazakhstan state technical university, Ust-Kamenogorsk, Kazakhstan, ORCID ID: 0000-0002-9649-2315

### Article history

Received 20.04.2019  
Accepted 25.05.2019  
Available online 04.07.2019

### Keywords

Road roller  
shell  
force  
stress

### Abstract

The article is devoted to solving the fundamental and applied problem of nonlinear structural mechanics of machines by introducing into the drum two additional stop cylinders with supporting rollers at the end and adjustable length, providing a given elliptical or circular shape of a flexible shell with a smoothly variable geometry in the area of its contact with compacted pavement material. Compaction of soil, gravel and asphalt concrete in the sphere of road is not only an integral part of the technological process of the roadbed, road foundation and surface construction, but it is actually the main operation to ensure their strength, stability and durability. The quality, cost and speed of road construction, the possibility of using fundamentally new technologies, structures and materials is largely determined by the availability of modern road machinery.

DOI: 10.30657/pea.2019.23.05

JEL: L69, M11

## 1. Introduction

One of the main directions of scientific and technological progress is the creation and introduction of new equipment, the improvement of the existing one, as well as the improvement of its quality, reliability, durability with minimal material consumption and cost per unit of power.

A summary of the issue of quantifying the carrying capacity of the shell can only be done after joint mathematical modeling of the physical process of interaction between the roller and the material of the sealing coating and solving the problem of local elastic stability of a thin-walled cylindrical shell (shell) under local contact pressure" (Abdeev et al., 2011; Sakimov et al., 2018).

The article presents the analysis of the behavior of the deformable roller shell of the road roller, and the material to be compacted under the compacting roller of the road roller (Dudkin et al., 2006), in which the rigid circular shell of the roller is replaced by a forcefully deformable elliptical shape, which, unlike the circular design, allows variation, adjustment and optimization of the impact of the road roller on the material to be compacted.

## 2. Mathematical Model

This article is devoted to solving this fundamental and applied problem of nonlinear structural mechanics of machines (Birger et al., 1979) by introducing into the drum two additional stop cylinders with supporting rollers at the end and adjustable length, providing a given elliptical or circular shape of a flexible shell with a smoothly variable geometry (Dudkin et al., 2006; Abdeev et al., 2012 et al., 2018) in the area of its contact with compacted pavement material, based on:

- 1) the closest and symmetrical positioning at the same distance  $l_p \geq C$  of roller support-cylinders, the length of which in the design scheme of figure 1 is almost identical to the width  $B$  of the roller (figure 2), and their rigidity, according to size, is much more than deformability of the flexible shell having the thickness  $\delta \ll d_p$  - the diameter of the rollers;
- 2) the distribution locality of contact pressure functions  $q_c = q_c(x_1), q_p = q_p(x_1)$ , at which the lengths of the corresponding projections  $C, C_p$  pologic shell arcs in contact with the material of the coating being

compacted are comparable to its thickness  $\delta$ , and in this connection, as is known (Ponomarev and Andreeva, 1980), in small areas of the simulated thin-walled system bounded by  $2C \times B$  areas (stationary roller, figure 1) and  $C_{II} \times B$  (rotating movable roller, figure 1) obvious conditions are observed (Sakimov et al., 2018; Bostanov et al., 2018)

$$\frac{1}{80} < \frac{\delta}{2 \cdot C} < \frac{1}{5}, \quad \frac{1}{80} < \frac{\delta}{C_p} < \frac{1}{5}, \quad (1)$$

confirming the low probability of clipping, since within the constraints (1) the shell will deform like a cylindrical flat shell-panel of relatively large thickness  $\delta$  and a small bend (within the limits of size  $\delta$ ), in which (Kolkunov, 1972)

$$y_{\max} < \frac{2 \cdot l_p}{5} = 0,4 \cdot l_p. \quad (2)$$

At the same time, in order to guarantee the tuning of the considered structure in order to exclude the possibility of local deformations from the reactive distributed forces  $q_c, q_p$  (n), it is necessary to solve the stability test proble. For its mathematical formulation, with a margin of rigidity mand bearing capacity, an idealized model of a linearly elastic homogeneous isotropic rectangular plate-panel with a plan size  $2l_p \times B$  (Fig. 2) is used with an initial bend  $y_1 = y(x_1)$ , approximated by circle or ellipse functions and fixed projections  $l_p \geq C = \max$ , symmetrically located arcs  $S_p$ . At the same time, for the calculated pressure  $q_p(x_1)$  with the greatest extremum  $q = \max$  (Fig. 2) the functional expression of Hertz-Shtererman is taken (Sakimov et al., 2018)

$$q_p = q_p(x_1) = \frac{q}{l_p} \sqrt{l_p^2 - x_1^2} \geq 0, \quad q < q_{kv}, \quad (3)$$

changing on a plane  $-l_p \leq x_1 \leq l_p, -0,5 B \leq z_1 \leq 0,5 B$  by the same even law as addition  $q_c = q_c(x_1)$ , in the case of a stationary drum (Fig. 1) while limiting the maximum value  $q < q_{kv}$  regulatory minimum safety factor  $[n_y] = 1,5$  for an ideal original shell surface (no dents)

$$n_y = \frac{q_{kv}}{q_{mp}} \geq [n_y] = 1,5 \quad (4)$$

in relation to the upper critical load  $q_{kv}$ , corresponding to the unacceptable phenomenon of flipping the shell to a new stationary equilibrium state with the formation of a local bend (Temirbekov et al., 2019)

Each mechanical system with the loss of stability can behave differently. A transition to a certain new equilibrium state usually takes place, which in the overwhelming majority of cases, is accompanied by large displacements, the appearance of plastic (residual) deformations or complete destruction. In relation to the considered road roller with flexible elastic shell (Dudkin et al., 2006; Abdeev et al., 2012), the listed negative factors lead to the impossibility of its further operation or to a significant reduction in the quality indicators of the fulfillment of its functional purpose. On this basis, the topic of this article is extremely relevant, innovative and promising.

The corresponding applied physical and mathematical problem of an elastically deformable solid body is based on the fundamental system of two nonlinear fourth-order differential equations (Fig. 2).

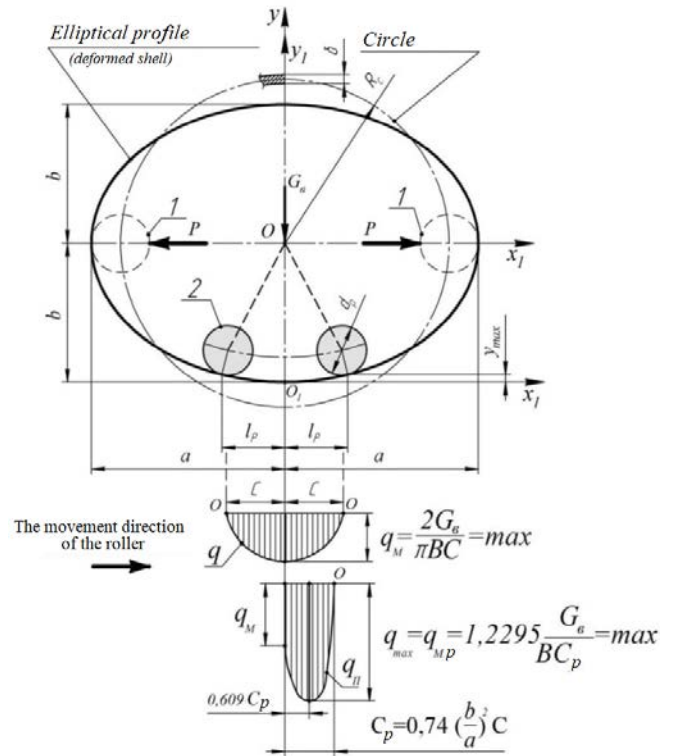
$$\left\{ \begin{aligned} \frac{E \cdot \delta^2}{12(1 - \mu^2)} \nabla^4 \omega &= \frac{\partial^2 \Phi}{\partial x_1^2} \cdot \frac{\partial^2 \omega}{\partial z_1^2} + \frac{\partial^2 \Phi}{\partial z_1^2} \left( \frac{\partial^2 \omega}{\partial x_1^2} + \frac{\partial^2 y_1}{\partial x_1^2} \right) - \\ &- 2 \frac{\partial^2 \Phi}{\partial x_1 \partial z_1} \cdot \frac{\partial^2 \omega}{\partial x_1 \partial z_1} + \frac{q}{\delta \cdot l_p} \sqrt{l_p^2 - x_1^2}, \\ \frac{1}{E} \nabla^4 \Phi &= \left( \frac{\partial^2 \omega}{\partial x_1 \partial z_1} \right)^2 - \\ &- \frac{\partial^2 \omega}{\partial x_1^2} \cdot \frac{\partial^2 \omega}{\partial z_1^2} - \frac{\partial^2 \omega}{\partial z_1^2} \cdot \frac{\partial^2 y_1}{\partial x_1^2}, \end{aligned} \right. \quad (5)$$

$$\quad (6)$$

where  $E, \mu$  – respectively, the modulus of elasticity and Poisson’s ratio of the shell material (structural spring steel (Abdeev et al., 2012));

$x_1, z_1$  – local coordinates of an arbitrary point of the median surface of the shell, varying within

$$-l_p \leq x_1 \leq l_p \geq C = \max > C_p, -0,5 B \leq z_1 \leq 0,5 B; \quad (7)$$



1 - Support rollers at the end of the hydraulic cylinders, creating and supporting with the help of forces  $P$ , an elliptical shape of the shell, 2 - Hydraulic cylinders with roller bearings of cylindrical type, providing a predetermined shape of the shell and increasing its bearing capacity (local stability) in the area of action of reactive distributed loads  $q, q_p$

Fig. 1. Design and design diagram of a general form with contact pressure diagrams  $q$  and  $q_p$



$$\omega(\pm l_p) = 0, \left[ \frac{d\omega}{dx_1} \right]_{x_1=\pm l_p} = f \left( -\frac{4x_1}{l_p^2} + \frac{x_1^3}{l_p^4} \right) \Big|_{x_1=\pm l_p} = 0, \quad (21)$$

where the maximum calculated chord length  $l_p$ , identical to the distance between roller bearings (Fig. 1), is found, according to (8) and guided by (Sakimov and Eleukenov, 2012; Sakimov et al., 2018).

$$\begin{aligned} l_p \geq C = \max &= 1,0925 a_p \cdot \sqrt{\frac{G_B}{E_K \cdot b_p \cdot B}} = \\ &= 1,0925 \cdot 1,0954 \cdot R_c \sqrt{\frac{G_B}{E_K \cdot 0,9 R_c \cdot B}} = \\ &= 1,26146 \cdot R_c \sqrt{\frac{G_B}{E_K \cdot R_c \cdot B}} \end{aligned} \quad (22)$$

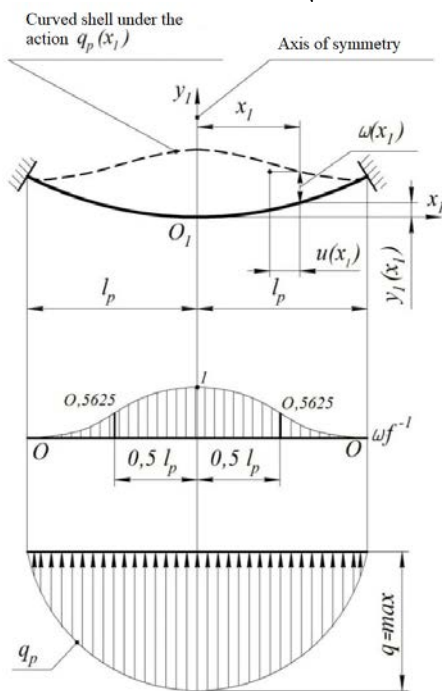


**Fig. 3.** Arbitrary section  $z_1$ , rigidly clamped on straight sides, element of Figure 2 and deflection  $\omega \cdot f^{-1}$  from the calculated contact pressure  $q_p$

with constructive-permissible dimensions of the semi axes of the ellipse (11) (Abdeev et al., 2012)

$$a_p = 1,0954 \cdot R_c, b_p = 0,9 \cdot R_c \quad (23)$$

with extreme eccentricity (12)

$$\xi = \xi_p = 0,57 \quad (24)$$

To solve the system (17), (19), the necessary derivatives of the functions  $\omega(x_1), y_1(x_1)$ , are preliminarily determined based on dependencies (10), (20), (21) and reference information (Doudkin et al., 2013):

$$\frac{d\omega}{dx_1} = 4f \left( -\frac{x_1}{l_p^2} + \frac{x_1^3}{l_p^4} \right), \quad (25)$$

$$\frac{d^2\omega_1}{dx_1^2} = 4f \left( -\frac{1}{l_p^2} + \frac{3x_1^2}{l_p^4} \right), \quad (26)$$

$$\frac{d^4\omega_1}{dx_1^4} = 24 \frac{f}{l_p^4} = \text{const}, \quad (27)$$

$$\left. \begin{aligned} \frac{dy_1}{dx_1} &= -\frac{b \left( -\frac{2x_1}{a^2} \right)}{2 \sqrt{1 - \frac{x_1^2}{a^2}}} \approx \frac{bx}{a^2}, \\ \frac{d^2y_1}{dx_1^2} &= \frac{b}{a^2 \left( 1 - \frac{x_1^2}{a^2} \right)^{3/2}} \approx \frac{b}{a^2} = \text{const}. \end{aligned} \right\} \quad (28)$$

The first derivative (25) is substituted into the deformation relation (19) and by direct integration (Doudkin et al., 2013) the second kinematic component is found (Fig. 3):

$$u = u(x_1) = \int \left[ \frac{A}{E} - \frac{1}{2} \left( \frac{d\dot{u}}{dx_1} \right)^2 \right] \cdot dx_1 + C = \frac{A}{E} x_1 - 8f^2 \left( \frac{x_1^3}{3l_p^3} - 2 \frac{x_1^5}{5l_p^5} + \frac{x_1^7}{7l_p^7} \right), \quad (29)$$

where is an arbitrary constant  $C = 0$  from the odd-odd condition  $u(0)=0$  function  $u(x_1)$ .

To calculate the constant A, the third homogeneous boundary equality was formulated (Kolkunov, 1972):

$$\begin{aligned} u(\pm l_p) &= \pm \left[ \frac{A}{E} l_p - 8f^2 \left( \frac{1}{3l_p} - \frac{2}{5l_p^3} + \frac{1}{7l_p^5} \right) \right] = 0, \Rightarrow \\ A &= \frac{64E}{105} \cdot \frac{f^2}{l_p^2}. \end{aligned} \quad (30)$$

Further, the procedure of the Bubnov-Galerkin method is applied to the one-dimensional equation (17) in the form of the corresponding integral-differential relation

$$\begin{aligned} 2 \int_0^{l_p} \left[ \frac{E \cdot \ddot{a}^2}{12(1 - \dot{\epsilon}^2)} \cdot \frac{d^4 \dot{u}}{dx_1^4} - \frac{64E}{105} \cdot \frac{f^2}{l_p^2} \left( \frac{d^2 \dot{u}}{dx_1^2} + \frac{d^2 y_1}{dx_1^2} \right) - \frac{q}{\dot{a}} \cdot \right. \\ \left. \cdot \sqrt{1 - \frac{x_1^2}{l_p^2}} \times \left( 1 - \frac{x_1^2}{l_p^2} \right)^2 \cdot dx_1 = 0, \end{aligned} \quad (31)$$

taking into account expressions (20), (26) - (28), (30) and the symmetry of the design scheme of Figure 3, and the tables (Doudkin et al., 2013) are used to calculate the integrals included in (31), after a valid simplification of the functional formula  $y_1(x_1)$ , subject to the restrictions (10) (Temirbekov et al., 2019) and its derivatives (28):

$$\begin{aligned} y_1 = y_1(x_1) &= b \left( 1 - \sqrt{1 - \frac{x_1^2}{a^2}} \right) \approx b \left[ 1 - \left( 1 - \frac{x_1^2}{2a^2} \right) \right] = \\ &= \frac{b \cdot x_1^2}{2a^2}, \Rightarrow \frac{d^2 y_1}{dx_1^2} = \frac{b}{a^2} \text{ (see (28));} \end{aligned} \quad (32)$$

$$\int_0^{l_p} \frac{d^4 \dot{u}}{dx_1^4} \left( 1 - \frac{2x_1^2}{l_p^2} + \frac{x_1^4}{l_p^4} \right) \cdot dx_1 = \frac{24f}{l_p^4} \left( x_1 - \frac{2x_1^3}{3l_p^2} + \frac{x_1^5}{5l_p^4} \right) \Big|_0^{l_p} = \frac{64 \cdot f}{5l_p^3}, \quad (33)$$

$$\int_0^{l_p} \frac{d^2 \dot{u}}{dx_1^2} \cdot \left( 1 - \frac{x_1^2}{l_p^2} \right)^2 \cdot dx_1 = 4f \int_0^{l_p} \left( -\frac{1}{l_p^2} + \frac{3x_1^2}{l_p^4} \right) \cdot \left( 1 - \frac{2x_1^2}{l_p^2} + \frac{x_1^4}{l_p^4} \right) \cdot dx_1 = \quad (34)$$

$$= 4f\left(-\frac{x_1}{l_p^2} + \frac{5 \cdot x_1^3}{3 \cdot l_p^4} - \frac{7 \cdot x_1^5}{5 \cdot l_p^6} + \frac{3 \cdot x_1^7}{7 \cdot l_p^8}\right)\Big|_0^{l_p} = -\frac{128 \cdot f}{105 \cdot l_p^5},$$

$$\begin{aligned} \int_0^{l_p} \frac{d^2 y_1}{dx_1^2} \left(1 - \frac{x_1^2}{l_p^2}\right)^2 \cdot dx_1 &= \\ &= \frac{b}{a^2} \int_0^{l_p} \left(1 - \frac{2x_1^2}{l_p^2} + \frac{x_1^4}{l_p^4}\right) \cdot dx_1 = \\ &= \frac{b}{a^2} \left(x_1 - \frac{2x_1^3}{3l_p^2} + \frac{x_1^5}{5l_p^4}\right)\Big|_0^{l_p} = \frac{8 \cdot b \cdot l_p}{15 \cdot a^2}, \end{aligned} \quad (35)$$

$$\begin{aligned} \int_0^{l_p} \left(1 - \frac{2x_1^2}{l_p^2} + \frac{x_1^4}{l_p^4}\right)^2 \cdot \sqrt{1 - \frac{x_1^2}{l_p^2}} \cdot dx_1 &= \\ &= \int_0^{l_p} \sqrt{1 - \frac{x_1^2}{l_p^2}} \cdot dx_1 - \\ &- \frac{2}{l_p^2} \int_0^{l_p} x_1^2 \cdot \sqrt{1 - \frac{x_1^2}{l_p^2}} \cdot dx_1 + \frac{1}{l_p^4} \int_0^{l_p} x_1^4 \cdot \sqrt{1 - \frac{x_1^2}{l_p^2}} \cdot dx_1 = \\ &= \frac{l_p}{2} \arcsin \frac{x_1}{l_p} \Big|_0^{l_p} - \frac{l_p}{4} \arcsin \frac{x_1}{l_p} \Big|_0^{l_p} + \frac{l_p}{16} \arcsin \frac{x_1}{l_p} \Big|_0^{l_p} = \frac{5 \cdot \pi \cdot l_p}{32} \end{aligned} \quad (36)$$

Substituting (33) - (36) into algebraic equation (31), we obtain the classical cubic dependence  $q(f)$  (Kolkunov, 1972) between the extremum  $q$  of reactive pressure  $q_p = q_p(x_1)$  (Fig. 2) and deflection (20) (Fig. 3) with  $\pi = 3,1416$ :

$$f = \omega(0) = \omega_{max}: \quad (37)$$

$$\begin{aligned} q = q(f) &= 1,5137 \cdot \frac{E \cdot \delta}{l_p^4} \cdot f^3 - \\ &- 0,6622 \cdot \frac{E \cdot b \cdot \delta}{l_p^2 \cdot a^2} \cdot f^2 + \frac{2,173}{1 - \mu^2} \cdot \frac{E \cdot \delta^3}{l_p^4} \cdot f \end{aligned} \quad (38)$$

In order to increase the level of generalization and universality of the practical application of the derived formula (38), according to the method (Kolkunov, 1972), dimensionless physical and geometric characteristics are introduced:

$$\zeta = \frac{f}{\delta}, \quad q^* = \frac{q}{E} \left(\frac{l_p}{\delta}\right)^4 \quad (39)$$

$$\lambda = \frac{b \cdot l_p^2}{a^2 \cdot \delta} = \frac{2 \cdot l_p^2 \cdot E(\xi) \cdot \sqrt{1 - \xi^2}}{\pi \cdot R_c \cdot \delta}; \quad (40)$$

where, according to (12) and (Abdeev et al., 2012),

$$b = a \sqrt{1 - \xi^2}, \quad a = \frac{\pi \cdot R_c}{2 \cdot E(\xi)}, \quad (41)$$

where  $E(\xi)$  – elliptic integral of the second kind in the Legendre form (Doudkin et al., 2013), for which calculation the reference tables were compiled. The transformed relation (38), including parameters (39), (40), takes a more compact form.

$$q^* = q^*(\zeta) = 1,5137 \zeta^3 - 0,6622 \lambda \zeta^2 + \frac{2,173}{1 - \mu^2} \zeta \quad (42)$$

For any values  $\lambda > 0$  curve (42) always has one inflection point, which has the coordinate  $\zeta_0$ , determined from the equality of zero of the second derivative (Doudkin et al., 2013):

$$\left[\frac{d^2 q^*}{d\zeta^2}\right]_{\zeta=\zeta_0} = 9,0822 \zeta_0 - 1,3244 \lambda = 0, \quad (43)$$

where it comes from:

$$\zeta_0 = \frac{1,3244}{9,0822} \lambda = 0,1458 \cdot \lambda. \quad (44)$$

Realizing condition  $\frac{dq^*}{d\zeta} = 0$ , two values are found  $\zeta_B, \zeta_n$ , corresponding to the top  $q_{kv}^*$  and bottom  $q_{kn}^*$  (after clicking (Kolkunov, 1972)) critical pressure on the shell (Fig. 2):

$$\left[\frac{dq^*}{d\zeta}\right]_{\zeta=\zeta_n} = 4,5411 \zeta_n^2 - 1,3244 \cdot \lambda \cdot \zeta_n + \frac{2,173}{1 - \mu^2} = 0, \Rightarrow \quad (45)$$

$$\zeta_n = 0,145825 \cdot \lambda \mp \sqrt{0,021265 \lambda^2 - \frac{0,47852}{1 - \mu^2}} \quad (46)$$

Click area border  $\lambda_{gr}$  adequate to the case when the function (42) has an inflection point containing a horizontal tangent, when the root expression in (46) vanishes,  $\Rightarrow$

$$\lambda_{gr} = \frac{4,7437}{\sqrt{1 - \mu^2}} = const; \quad (47)$$

and, as a consequence of (46),

$$\zeta_B^{(gr)} = \zeta_n^{(gr)} = \zeta_{gr} = 0,145825 \cdot \lambda_{gr} = \frac{0,69175}{\sqrt{1 - \mu^2}} = const \quad (48)$$

Subsequent analytical testing of formulas (22), (42), (44), (46) - (48) are performed in numerical form using specific data given in published papers (Abdeev et al., 2018) for a circular outline of the (K) with  $\xi = 0$ ,  $E(0) = 1,5708$  and in the case of an elliptical shape (E) of the surface of the drum, when  $\xi = \xi_p = 0,57$ ,  $E(\xi_p) = E(0,57) = 1,434$ . The material of construction is spring-spring steel 60C2XA (Doudkin et al., 2013) having:  $E = 1,96 \cdot 10^5 \text{ MPa}$   $\left(\frac{N}{\text{mm}^2}\right)$ , Poisson's ratio  $\mu = 0,256$  and yield strength  $\sigma_T = 2270 \text{ MPa}$   $\left(\frac{N}{\text{mm}^2}\right)$ . As the linear dimensions of the shell are taken (Fig. 1 and 2)  $\delta = 6,5 \text{ mm}$ ,  $R_c = 600 \text{ mm}$ ,  $B = 1400 \text{ mm}$ ,  $l_p = 90 \text{ mm}$  at rated axle load of the roller  $G_B = 42500 \text{ N}$  and deformation module  $E_K$  sealing coating (Sakimov et al., 2018):

$$E_K = 8; 20; 30; 65; 116 \text{ MPa} \left(\frac{N}{\text{mm}^2}\right). \quad (49)$$

Check the constructive-technological background (22), which regulates a fixed geometric characteristic  $l_p = 90 \text{ mm}$  (Fig. 1-3):

$$\begin{aligned} l_p = 90 \text{ mm} > C = 1,26146 \cdot R_c \sqrt{\frac{G_B}{E_K^{(\min)} \cdot R_c \cdot B}} &= \\ &= 1,26146 \cdot 600 \sqrt{\frac{42500}{8 \cdot 600 \cdot 1400}} = 60,2 \text{ mm}, \end{aligned} \quad (50)$$

when  $E_K^{(\min)} = 8 \frac{N}{\text{mm}^2}$ , according to (49).

Figure 4 shows the graphs of the functional ratios of the maximum contact pressure  $q_{mp} = q_{mp}(E_K)$  for a rolling roller (Fig. 1), constructed according to the formulas (Sakimov et al., 2018) of figure 1 using dependencies (8), (22), (23) and the quantitative information of Table 1:

- at  $\xi = 0$ ,  $E(0) = 1,5708$  (round drum - "K")

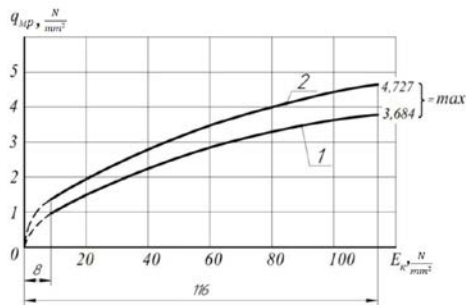
$$q_{mp}^{(K)} = 1,2295 \frac{G_B}{B \cdot 0,74 C} = 1,2295 \frac{G_B \sqrt{E_K \cdot R_c \cdot B}}{B \cdot 0,74 \cdot 1,0925 \cdot R_c \sqrt{G_B}} = \frac{1,2295}{0,74 \cdot 1,0925} \cdot \sqrt{\frac{G_B \cdot E_K}{B \cdot R_c}} = 1,5208 \cdot \sqrt{\frac{42500 \cdot E_K}{1400 \cdot 600}} = 0,34208 \cdot \sqrt{E_K}$$

- at  $\xi = 0,57$ ,  $E(0,57) = 1,434$  (extreme - elliptical shape of the shell - "E")

$$q_{mp}^{(E)} = 1,2295 \frac{G_B \sqrt{E_K \cdot R_c \cdot B}}{B \cdot 0,74 \cdot \left(\frac{0,9}{1,0954}\right)^2 \cdot R_c \sqrt{G_B}} = 1,9511 \cdot \sqrt{\frac{G_B \cdot E_K}{B \cdot R_c}} = 1,9511 \cdot \sqrt{\frac{42500 \cdot E_K}{1400 \cdot 600}} = 0,43887 \cdot \sqrt{E_K}$$

**Table 1** - Numerical data on functions (51), (52)

Shell Perimeter Shape	$E_K \frac{N}{mm^2}$	0	8	20	30	65	116
1 - Circle	$q_{mp}^{(K)} \frac{N}{mm^2}$	0	0,968	1,53	1,874	2,758	3,684
2 - Ellipse	$q_{mp}^{(E)} \frac{N}{mm^2}$	0	1,241	1,963	2,404	3,538	4,727



1 - For a shell in the form of a circular cylinder; 2 - For elliptical shell outline

**Fig. 4.** Graphic interpretation of the formulas (51), (52)

From equality (48), taking into account (23), (39), (40), (42), (47), we find the boundary thickness  $\delta_{gr}$ , as well as maximum deflection  $f_{gr}$  and pressure  $q_{gr}$ , to which a click or local loss of stability will occur, accompanied by a change in the shape of the element of the cylindrical shell (Fig. 1 and 2) in the form of a local dent (Fig. 3):

$$\lambda_{gr} = \frac{b \cdot l_p^2}{a^2 \cdot \delta_{gr}} = \frac{4,7437}{\sqrt{1-(0,256)^2}} = 4,9072; \quad (53)$$

$$\zeta_{gr} = \frac{f_{gr}}{\delta_{gr}} = 0,145825 \cdot \lambda_{gr} = 0,145825 \cdot 4,9072 = 0,7156; \quad (54)$$

$$q_{gr}^* = 1,5137 \cdot \zeta_{gr}^3 - 0,6622 \cdot \lambda_{gr} \cdot \zeta_{gr}^2 + \frac{2,173}{\sqrt{1-(0,256)^2}} \cdot \zeta_{gr} = 1,51137 \cdot (0,7156)^3 - 0,6622 \cdot 4,9072 \cdot (0,7156)^2 + 2,2479 \cdot 0,7156 = 0,4984; \quad (55)$$

$$q_{gr}^* = \frac{q_{mp}}{E} \cdot \left(\frac{l_p}{\delta_{gr}}\right)^4 = 0,4984; \quad (56)$$

where:

- for round drum with  $a = b = R_c = 600 \text{ mm}$

$$\delta_{gr}^{(K)} = \frac{b \cdot l_p^2}{4,9072 \cdot a^2} = \frac{l_p^2}{4,9072 \cdot R_c} = \frac{90^2}{4,9072 \cdot 600} = 2,75 \text{ mm}, \quad (57)$$

$$f_{gr}^{(K)} = \delta_{gr}^{(K)} \cdot 0,7156 = 2,75 \cdot 0,7156 = 1,97 \text{ mm}, \quad (58)$$

$$q_{gr}^{(K)} = 0,4984 \cdot E \cdot \left(\frac{\delta_{grp}^{(K)}}{l_p}\right)^4 = 0,4984 \cdot 196000 \cdot \left(\frac{2,75}{90}\right)^4 = 0,085 \frac{N}{mm^2}; \quad (59)$$

- for an elliptical shell surface

$$a = a_p = 1,0954 \cdot R_c \text{ and } b = b_p = 0,9 \cdot R_c$$

$$\delta_{gr}^{(E)} = \frac{0,9 \cdot R_c \cdot l_p^2}{4,9072 \cdot (1,0954 \cdot R_c)^2} = \frac{0,9 \cdot 90^2}{4,9072 \cdot (1,0954)^2 \cdot 600} = 2,06 \text{ mm}, \quad (60)$$

$$f_{gr}^{(E)} = \delta_{gr}^{(E)} \cdot 0,7156 = 2,06 \cdot 0,7156 = 1,47 \text{ mm}, \quad (61)$$

$$q_{gr}^{(E)} = 0,4984 \cdot E \cdot \left(\frac{\delta_{gr}^{(E)}}{l_p}\right)^4 = 0,4984 \cdot 196000 \cdot \left(\frac{2,06}{90}\right)^4 = 0,027 \frac{N}{mm^2} \quad (62)$$

Let us consider in more detail dependencies (39), (40), (42), (44) with the actual thickness of the shell (Abdeev et al., 2012)  $\delta = 6,5 \text{ mm} > \delta_{gr}$ , when the phenomenon of clicking is impossible:

- for round-shaped drum (K)
- with elliptical shell (E)

$$\lambda_E = \frac{0,9 \cdot R_c \cdot l_p^2}{6,5 \cdot (1,0954 \cdot R_c)^2} = \frac{0,9 \cdot 90^2}{6,5 \cdot (1,0954)^2 \cdot 600} = 1,559, \quad (66)$$

$$\zeta_0^{(E)} = 0,1458 \cdot \lambda_E = 0,1458 \cdot 1,559 = 0,2273, \quad (67)$$

$$q_0^{*(E)} = 1,5137 \cdot (0,2273)^3 - 0,6622 \cdot 1,559 \cdot (0,2273)^2 + 2,3254 \cdot 0,2273 = 0,493. \quad (68)$$

Since, as already noted, at  $\delta=6.5$  mm, loss of stability is excluded, the assessment of its bearing capacity is of decisive importance for the normal elastic operation of the shell, (Temirbekov et al., 2019)

$$\delta_{max} \leq \sigma_T, \quad (69)$$

at the highest normal stress and yield strength of the material  $\sigma_T = 2270$  MPa  $\left(\frac{N}{mm^2}\right)$  (Abdeev Bet al., 2012). Solving this issue will require a preliminary determination of the operating maximum dimensionless characteristics:

$$q_M^{*(K)}, q_M^{*(E)}, \zeta_{MK}, \zeta_{ME} \text{ при } q_{MP}^{(K)} = 3,684 \frac{N}{mm^2} = max$$

$q_{MP}^{(E)} = 4,727 \frac{N}{mm^2} = max$  (see table 1 and figure 4), based on relations (39), (42), (63), (66):

$$q_M^{*(K)} = \frac{q_{MP}^{(K)}}{E} \cdot \left(\frac{l_p}{\delta}\right)^4 = \frac{3,684}{196000} \cdot \left(\frac{90}{6,5}\right)^4 = 0,6908, \quad (70)$$

$$q_M^{*(E)} = \frac{q_{MP}^{(E)}}{E} \cdot \left(\frac{l_p}{\delta}\right)^4 = \frac{4,727}{196000} \cdot \left(\frac{90}{6,5}\right)^4 = 0,8864; \quad (71)$$

$$\begin{cases} 1,5137 \cdot \zeta_{MK}^3 - 0,6622 \cdot 2,0769 \cdot \zeta_{MK}^2 + \\ + 2,3254 \cdot \zeta_{MK} = q_M^{*(K)} = 0,6908, \end{cases} \quad (72)$$

$$\begin{cases} 1,5137 \cdot \zeta_{ME}^3 - 0,6622 \cdot 1,559 \cdot \zeta_{ME}^2 + \\ + 2,3254 \cdot \zeta_{ME} = q_M^{*(E)} = 0,8864; \end{cases} \quad (73)$$

whence by the method of selection or by Cardan's formulas (Doudkin et al., 2013),

$$\zeta_{MK} = 0,3398, \zeta_{ME} = 0,4109, \quad (74)$$

and the real greatest deflections  $f_K, f_E$  (Fig. 3) will have the following meanings:

$$f_K = \zeta_{MK} \cdot \delta = 0,3398 \cdot 6,5 = 2,21 \text{ mm}, \quad (75)$$

$$f_E = \zeta_{ME} \cdot \delta = 0,4109 \cdot 6,5 = 2,67 \text{ mm} \quad (76)$$

Visual illustration of the function (42) approximated by analytic expressions:

$$q^{*(K)} = 1,5137\zeta^3 - 1,37534\zeta^2 + 2,3254\zeta \quad (77)$$

$$q^{*(E)} = 1,5137\zeta^3 - 1,03234\zeta^2 + 2,3254\zeta \quad (78)$$

respectively, for circular (K) and ellipsoid (E) shells with  $\delta = 6,5$  mm, presented in figure 5. Dependency graphs  $q^{*(K)}(\zeta), q^{*(E)}(\zeta)$  constructed according to table 2 and characteristic values (64), (65), (67), (68), (70), (71), (74).

**Table 2.** Numerical information on the functional curves of Figure 5

Shell Form	$\zeta$	0	0,1	0,2	0,3	0,4	0,5
1 - Circle	$q^{*(K)}$	0	0,2203	0,4222	0,6147	0,807	1,008
2 - Ellipse	$q^{*(E)}$	0	0,2237	0,4359	0,6456	0,8619	1,094

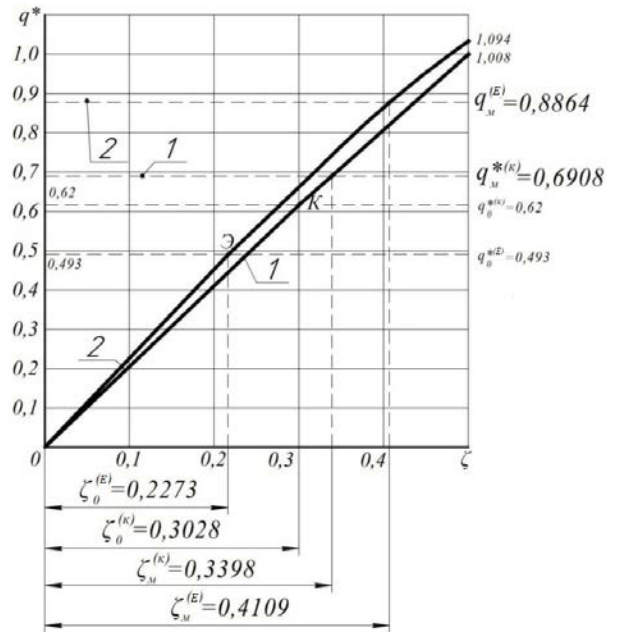


**Fig. 5.** Graphs of dimensionless functional relationships (77) and (78)

### 3. Conclusion

Having absolute extreme deformations (75), (76) – deflections  $f_K, f_M$ , it is possible to define:

- local compressive stresses  $\sigma_{x_1}^{(K)}, \sigma_{x_1}^{(E)}$  according to the general formula (16) taking into account (30):

$$\begin{aligned} \sigma_{x_1}^{(K)} &= \frac{64 \cdot E}{105} \cdot \frac{f_K^2}{l_p^2} = \\ &= \frac{64 \cdot 196000}{105} \cdot \left(\frac{2,21}{90}\right)^2 = 72,04 \frac{N}{mm^2}, \end{aligned} \quad (79)$$

$$\begin{aligned} \sigma_{x_1}^{(E)} &= \frac{64 \cdot E}{105} \cdot \frac{f_E^2}{l_p^2} = \\ &= \frac{64 \cdot 196000}{105} \cdot \left(\frac{2,67}{90}\right)^2 = 105,14 \frac{N}{mm^2}; \end{aligned} \quad (80)$$

- highest normal stresses  $\sigma_u^{(K)} = \sigma_u^{(K)}(x_1), \sigma_u^{(E)} = \sigma_u^{(E)}(x_1)$  from local cylindrical bend in design sections  $x_1 = 0, x_1 = \pm l_p = \pm 90$  mm (Fig. 3), applying the differen-

tial ratio (Ponomarev et al., 1980; Bostanov et al., 2018) and the second derivative (26) of the function  $\omega(x_1)$ :

$$\sigma_u = \sigma_u(x_1) = -\frac{E \cdot \delta}{2(1-\mu^2)} \cdot \frac{d^2\omega}{dx_1^2}, \Rightarrow \quad (81)$$

$$\begin{aligned} \sigma_u^{(k)}(0) &= -\frac{E \cdot \delta}{2(1-\mu^2)} \cdot \left(-\frac{4f_k}{l_p^2}\right) = \frac{2 \cdot E \cdot \delta \cdot f_k}{(1-\mu^2)l_p^2} = \\ &= \frac{2 \cdot 196000 \cdot 6,5 \cdot 2,21}{[1 - (0,256)^2] \cdot 90^2} = 744 \frac{N}{mm^2}, \end{aligned} \quad (82)$$

$$\begin{aligned} \sigma_u^{(E)}(0) &= \frac{2 \cdot E \cdot \delta \cdot f_3}{(1-\mu^2)l_p^2} = \frac{2 \cdot 196000 \cdot 6,5 \cdot 2,67}{[1 - (0,256)^2] \cdot 90^2} = \\ &= 898,8 \frac{N}{mm^2}; \end{aligned} \quad (83)$$

$$\begin{aligned} \sigma_u^{(k)}(\pm l_p) &= -\frac{E \cdot \delta}{2(1-\mu^2)} \cdot \left(\frac{8f_k}{l_p^2}\right) = \\ &= -2\sigma_u^{(k)}(0) = -2 \cdot 744 = -1488 \frac{N}{mm^2}, \end{aligned} \quad (84)$$

$$\sigma_u^{(E)}(\pm l_p) = -2\sigma_u^{(E)}(0) = -2 \cdot 898,8 = -1797,6 \frac{N}{mm^2} \quad (85)$$

- common bending static stresses  $\sigma_{oi}^{(k)}(x_1), \sigma_{oi}^{(E)}(x_1)$  from shell deformation in case  $P \geq 0$  (figure 1) (Dudkin et al., 2012)

$$\sigma_{oi}^{(k)}(0) = \sigma_{oi}^{(k)}(\pm l_p) = 0 \quad (86)$$

at  $P = 0$ ;

$$\begin{aligned} \sigma_{oi}^{(E)} &= -\frac{6}{B \cdot \delta^2} \cdot \frac{E \cdot B \cdot \delta^3}{12(1-\mu^2) \cdot R_c} \left[ \frac{0,7502}{\left(1 - 0,2708 \frac{x_1^2}{R_c^2}\right)^{3/2}} - 1 \right] \\ &= \\ &= -\frac{E \cdot \delta}{2(1-\mu^2) \cdot R_c} \left[ \frac{0,7502}{\left(1 - 0,2708 \frac{x_1^2}{R_c^2}\right)^{3/2}} - 1 \right], \Rightarrow \end{aligned} \quad (87)$$

$$\begin{aligned} \sigma_{oi}^{(E)}(0) &= -\frac{196000 \cdot 6,5}{2[1 - (0,256)^2] \cdot 600} (0,7502 - 1) \\ &= 283,8 \frac{N}{mm^2}, \end{aligned} \quad (88)$$

$$\begin{aligned} \sigma_{oi}^{(E)}(\pm l_p) &= \\ &= -\frac{E \cdot \delta}{2(1-\mu^2) \cdot R_c} \left[ \frac{0,7502}{\left(1 - 0,2708 \frac{l_p^2}{R_c^2}\right)^{3/2}} - 1 \right] = \\ &= -\frac{196000 \cdot 6,5}{2(1 - (0,256)^2) \cdot 600} \left[ \frac{0,7502}{\left(1 - 0,2708 \left(\frac{90}{600}\right)^2\right)^{3/2}} - 1 \right] \\ &= 276 \frac{N}{mm^2}. \end{aligned} \quad (89)$$

Using the results of calculations (79), (80), (82) - (86), (88), (89), condition (69) is checked by neglecting the stress  $\sigma_N$  in the middle surface of the shell from  $P > 0$  (Fig. 1),

compared with the bending components, which are much more orders of magnitude  $\sigma_N$ , as proved in article (Abdeev et al., 2012):

- for the material in section  $x_1=0$  (Fig. 2 and 3)

$$\begin{aligned} \sigma_{max}^{(k)}(0) &= \sigma_{x_1}^{(k)} + \sigma_u^{(k)}(0) + \sigma_{oi}^{(k)}(0) = 72,04 + 744 + 0 \\ &= 816,04 \frac{N}{mm^2}, \end{aligned} \quad (90)$$

$$\begin{aligned} \sigma_{max}^{(E)}(0) &= \sigma_{x_1}^{(E)} + \sigma_u^{(E)}(0) + \sigma_{oi}^{(E)}(0) = \\ &= 105,14 + 898,8 + 283,8 = 1207,74 \frac{N}{mm^2}; \end{aligned} \quad (91)$$

- for sections  $x_1 = \pm l_p = 90 \text{ mm}$  (Figures 2, 3)

$$\begin{aligned} \sigma_{max}^{(k)}(\pm l_p) &= \sigma_{x_1}^{(k)} + \left| \sigma_u^{(k)}(\pm l_p) \right| + \sigma_{oi}^{(k)}(\pm l_p) = \\ &= 72,04 + 1488 + 0 = 1560,04 \frac{N}{mm^2}, \end{aligned} \quad (92)$$

$$\begin{aligned} \sigma_{max}^{(E)}(\pm l_p) &= \sigma_{x_1}^{(E)} + \left| \sigma_u^{(E)}(\pm l_p) + \sigma_{oi}^{(E)}(\pm l_p) \right| = \\ &= 105,14 + |-1797,6 + 276| = 1626,74 \frac{N}{mm^2}. \end{aligned} \quad (93)$$

Thus,

$$\left. \begin{aligned} \sigma_{max}^{(k)} &= \sigma_{max}^{(k)}(\pm l_p) = 1560,04 \frac{N}{mm^2} < \sigma_T = 2270 \frac{N}{mm^2}, \\ \sigma_{max}^{(E)} &= \sigma_{max}^{(E)}(\pm l_p) = 1626,74 \frac{N}{mm^2} < \sigma_T = 2270 \frac{N}{mm^2}, \end{aligned} \right\} \quad (94)$$

and the required elastic operation of this shell without unacceptable residual deformations is ensured with a large minimum margin reaching 28.3%, primarily due to the use of structural spring steel 60C2XA (Abdeev et al., 2012) with a high yield strength  $\sigma_T = 2270 \text{ MPa}$   $\left(\frac{N}{mm^2}\right)$  (Doudkin et al., 2013).

## Reference

- Abdeev, B.M., Dudkin, M.V., Sakimov, M.A., Eleukenov, M.T., 2012. *Applied theory of assessing the strength of the steel shell of the roller of a road roller with a change in the curvature of the cylindrical guide*. Vestnik, D., Serikbaev EKSTU. - Ust-Kamenogorsk: 4, 2011, 27-36 (Part 1); 1, 35-45 (Part 2).
- Birger, I.A., Shorr, B.F., Iosilevich, G.B., 1979. *Calculation of the strength of machine parts: a Handbook*. - M, Mashinostroenie, 702.
- Bostanov, B.O., Temirbekov, E.S., Dudkin, M.V., Kim, A.I., 2018. *Mechanics-Mathematical Model of Conjugation of a Part of a Trajectory with Conditions of Continuity, Touch and Smoothness*. International Conference on Computer Aided Engineering. Computational and Information Technologies in Science, Engineering and Education, 9th International Conference, CITech 2018, Ust-Kamenogorsk, Kazakhstan. September 25-28, Proceedings. - P. 71-81. [https://doi.org/10.1007/978-3-030-12203-4\\_8](https://doi.org/10.1007/978-3-030-12203-4_8)
- Doudkin, M.V., Kim, A.I., Kim, V., 2019. *Application of FEM Method for Modeling and Strength Analysis of FEED Elements of Vibroscreen*, Proceedings of the 14th International Scientific Conference on Computer Aided Engineering, June 2018. Series: Lecture Notes in Mechanical Engineering. Wroclaw, Poland, 892.
- Doudkin, M.V., Kim, A.I., Kim, V., Mlynczak, M., Kustarev, G., 2018. *Computer Modeling Application for Analysis of Stress-strain State of Vibroscreen Feed Elements by Finite Elements Method*, Mathematical Modeling of Technological Processes International Conference, CITech

- 2018, Ust-Kamenogorsk, Kazakhstan, September 25-28, Proceedings. – P. 82-96. [https://doi.org/10.1007/978-3-030-12203-4\\_9](https://doi.org/10.1007/978-3-030-12203-4_9)
- Doudkin, M.V., Pichugin, S.Yu., Fadeev, S.N., 2013. *Contact Force Calculation of the Machine Operational Point*, Life Science Journal, 10, 246-250, doi:10.7537/marslsj1010s13.39.
- Doudkin, M.V., Pichugin, S.Yu., Fadeev, S.N., 2013. *Studying the Machines for Road Maintenance*, Life Science Journal, 10, 134-138. doi:10.7537/marslsj1012s13.24.
- Doudkin, M.V., Vavilov, A.V., Pichugin, S.Yu., Fadeev, S.N., 2013. *Calculation of the Interaction of Working Body of Road Machine with the Surface*, Life Science Journal, 10, 832-837. doi:10.7537/marslsj1012s13.133.
- Dudkin, M.V., Kuznetsov, P.S., Sakimov, M.A., Golovin, A.A., Kiyalbaev, A.K., 2006. *Roller of road roller*, Provisional Patent RK 18131. A.S. Of the Republic of Kazakhstan No. 51084, IPC E01C 19/26, E01C 19/23. Publ. No. 12; December 15.  
[http://nblib.library.kz/elib/library.kz/jurnal/Геология\\_03\\_2018/Sakimov%20\(str.207\)%20032018.pdf](http://nblib.library.kz/elib/library.kz/jurnal/Геология_03_2018/Sakimov%20(str.207)%20032018.pdf)
- Kolkunov, N.V., 1972. *Fundamentals of the calculation of elastic shells*, M.: Publishing house "High School", 296.
- Ponomarev, S.D., Andreeva, L.E., 1980. *The calculation of the elastic elements of machines and devices*, M.: Mashinostroenie, 326.
- Sakimov, M.A., Ozhikenova, A.K., Abdeyev, B.M., Dudkin, M.V., Ozhiken A.K., Azamatkyzy, S., 2018. *Finding allowable deformation of the road roller shell with variable curvature*, News of the national academy of sciences of the republic of Kazakhstan series of geology and technical sciences,3(429), 197 - 207.
- Temirbekov, E.S., Bostanov, B.O., Dudkin, M.V., Kaimov, S.T., Kaimov, A.T., 2019. *Combined Trajectory of Continuous Curvature*, Advances in Italian Mechanism Science.Proceedings of the Second International Conference of IFToMM Italy, Mechanisms and Machine Scienc. 68, 12-19, [https://doi.org/10.1007/978-3-030-03320-0\\_2](https://doi.org/10.1007/978-3-030-03320-0_2)

---

## 可变接触面几何形状的钢辊壳局部变形的力学和数学研究

---

### 關鍵詞

压路机  
贝壳  
力  
强调

### 摘要

本文致力于解决机器非线性结构力学的基本问题 and 应用问题，将两个附加的止动缸末端和可调长度引入到滚筒中，提供给定的椭圆形或圆形形状的柔性壳体，使其平滑在与压实路面材料接触的区域内的可变几何形状。

路面土壤，砾石和沥青混凝土的压实不仅是路基，路基和地面施工技术过程中不可或缺的一部分，而且实际上是确保其强度，稳定性和耐久性的主要操作。道路建设的质量，成本和速度，使用基本新技术，结构和材料的可能性在很大程度上取决于现代道路机械的可用性。

---